JOURNAL OF GUIDANCE, CONTROL, AND DYNAMICS
Vol. 17, No. 2, March–April 1994

# Riccati Equation Approaches for Small Gain, Positivity, and Popov Robustness Analysis

Emmanuel G. Collins Jr.*
*Harris Corporation, Melbourne, Florida 32902*
Wassim M. Haddad†
*Florida Institute of Technology, Melbourne, Florida 32901*
and
Lawrence D. Davis*
*Harris Corporation, Melbourne, Florida 32902*

**In recent years, small gain (or $H_\infty$) analysis has been used to analyze feedback systems for robust stability and performance. However, since small gain analysis allows uncertainty with arbitrary phase in the frequency domain and arbitrary time variations in the time domain, it can be overly conservative for constant real parametric uncertainty. More recent results have led to the development of robustness analysis tools, such as extensions of Popov analysis, that are less conservative. These tests are based on parameter-dependent Lyapunov functions, in contrast to the small gain test, which is based on a fixed quadratic Lyapunov function. This paper uses a benchmark problem to compare Popov analysis with small gain analysis and positivity analysis (a special case of Popov analysis that corresponds to a fixed quadratic Lyapunov function). The state-space versions of these tests, based on Riccati equations, are implemented using continuation algorithms. The results show that the Popov test is significantly less conservative than the other two tests and for this example is completely nonconservative in terms of its prediction of robust stability.**

## I. Introduction

ONE of the most important aspects of the control design and evaluation process is the analysis of feedback systems for robust stability and performance. Over the past several years, significant attention has been devoted to the use of small gain (or $H_\infty$) tests for robustness analysis.[1-5] However, it is well known that these tests can be very conservative since in the frequency domain the small gain test characterizes uncertainty with bounded gain but arbitrary phase, whereas in the time domain the small gain test characterizes uncertainty with arbitrary time variation.[5] This conservatism has led to the search for more accurate robustness tests. In particular, researchers have searched for tests that allow frequency domain uncertainty characterization to include phase bounding or time domain uncertainty characterization to include restrictions on the allowable time variations.

The small gain test is actually based on conventional or "fixed" quadratic Lyapunov functions that guarantee stability with respect to arbitrarily time-varying perturbations. Very recently, however, robustness tests have been developed that are based on quadratic Lyapunov functions that are a function of the parametric uncertainty, that is, "parameter-dependent Lyapunov functions."[6,7] In contrast to analysis based on a fixed quadratic Lyapunov function, these tests guarantee robust stability by means of a family of Lyapunov functions and do not apply to arbitrarily time-varying uncertainties. Hence, when the actual uncertainty is real and constant, these tests are less conservative than tests based on fixed quadratic Lyapunov functions.[6]

In this paper we use a benchmark problem to compare the Popov test,[2] based on a parameter-dependent Lyapunov function,[6,7] with the small gain[2] and positivity tests[2] that are based on fixed quadratic Lyapunov functions.[6,7] Each of the stability tests has graphical interpretations for the case of one-block, scalar uncertainty.[2] However, here we will emphasize the state-space tests that are based on Riccati equations and allow the development of robust $H_2$ performance bounds in addition to the determination of robust stability. We develop continuation algorithms for the special case of one-block, scalar uncertainty. The algorithm for Popov analysis additionally requires that a certain product $(\tilde{C}_0\tilde{B}_0)$ related to the uncertainty characterization be equal to zero. As will be seen in Sec. III, this condition holds for the parametric uncertainty under consideration. The algorithms are applied to analyze a feedback system for the benchmark system in which the controller was designed using the maximum entropy approach.[8]

The paper is organized as follows. Section II presents the linear system to be analyzed for robust stability and performance and gives the main theorems for the small gain, positivity, and Popov tests. Section III then considers the benchmark problem and formulates the feedback system to be analyzed in the format of Sec. II. Section IV applies the graphical tests to determine robust stability. Next, Sec. V develops continuation algorithms for a special case of the state-space tests and applies the algorithms to the benchmark problem. Finally, Sec. VI discusses the conclusions and directions for future work.

## II. Riccati Equation Characterizations for the Small Gain, Positivity, and Popov Theorems

We begin this section by establishing some basic notation and definitions. Let $\mathcal{R}$ denote the real numbers, and let $(\cdot)^T$ and $(\cdot)^*$ denote transpose and complex conjugate transpose. Furthermore, we write $\|\cdot\|_2$ for the Euclidean norm, $\|\cdot\|_F$ for the Frobenius norm, $\sigma_{\max}(\cdot)$ for the maximum singular value, $\mathrm{tr}(\cdot)$ for the trace operator, and $M \geq 0$ $(M > 0)$ to denote the fact that the hermitian matrix $M$ is nonnegative (positive) definite. The notation

$$G(s) \sim \left[\begin{array}{c|c} A & B \\ \hline C & D \end{array}\right] \tag{1}$$

Received Nov. 1, 1992; revision received June 18, 1993; accepted for publication June 19, 1993. 

*Staff Engineer, Government Aerospace Systems Division, MS 19/4849.
†Associate Professor, Department of Mechanical and Aerospace Engineering.

denotes that $G(s)$ is a transfer function corresponding to the state-space realization $(A, B, C, D)$, i.e., $G(s) = C(sI - A)^{-1} \times B + D$. The notation "$\overset{\min}{\sim}$" is used to denote a minimal realization. For asymptotically stable $G(s)$, define the $H_2$ and $H_\infty$ norms, respectively, where $\omega \in [0, \infty)$, as

$$\|G(s)\|_2^2 \triangleq \frac{1}{2\pi}\int_{-\infty}^{\infty} \|G(j\omega)\|_F^2 \, d\omega \tag{2a}$$

$$\|G(s)\|_\infty \triangleq \sigma_{\max}(G(j\omega)) \tag{2b}$$

A transfer function $G(s)$ is *bounded real* if 1) $G(s)$ is asymptotically stable and 2) $\|G(j\omega)\|_\infty \le 1$ for $\omega \in [0,\infty)$. Furthermore, $G(s)$ is called *strictly bounded real* if 1) $G(s)$ is asymptotically stable and 2) $\|G(j\omega)\|_\infty < 1$ for $\omega \in [0,\infty)$. Finally, note that if $G(s)$ is strictly bounded real, then $I - D^TD > 0$, where $D \triangleq G(\infty)$.

A square transfer function $G(s)$ is called *positive real* if 1) all poles of $G(s)$ are in the closed left half-plane and 2) $G(j\omega) + G^*(j\omega)$ is nonnegative definite for $\omega \in [0,\infty)$. A square transfer function $G(s)$ is called strictly positive real if 1) $G(s)$ is asymptotically stable and 2) $G(j\omega) + G^*(j\omega)$ is positive definite for $\omega \in [0,\infty)$. Finally, a square transfer function $G(s)$ is strongly positive real if it is *strictly positive real* and $D + D^T > 0$, where $D \triangleq G(\infty)$. (Note that in some of the literature "strongly positive real" as defined here is referred to as "strictly positive real.")

At this point, we consider a linear uncertain system of the form

$$\dot{\tilde{x}}(t) = (\tilde{A} - \tilde{B}_0F\tilde{C}_0)\tilde{x}(t) + \tilde{D}w(t), \qquad \tilde{x}(t) \in \mathcal{R}^{\tilde{n}} \tag{3}$$

$$z(t) = \tilde{E}\tilde{x}(t) \tag{4}$$

Note that the system (3) and (4) may denote a linear feedback system subject to an exogeneous disturbance signal $w(t)$. The individual elements of $z(t)$ may denote the performance variables, possibly including the actuation signals. The product $-\tilde{B}_0F\tilde{C}_0$ then denotes the parametric uncertainty (i.e., $\Delta\tilde{A}$). In particular, $\tilde{B}_0$ and $\tilde{C}_0$ are fixed matrices denoting the structure of the uncertainty and $F$ is an uncertain matrix. Here, it is assumed that for some nonnegative definite diagonal matrix $M$, $F \in \mathcal{F}_M^+$, or for some nonnegative scalar $\gamma$, $F \in \mathcal{F}_\gamma$ where

$$\mathcal{F}_M^+ \triangleq \{F \in \mathcal{R}^{m_0 \times m_0}: F \text{ is diagonal}, 0 \le F \le M\} \tag{5}$$

$$\mathcal{F}_\gamma \triangleq \{F \in \mathcal{R}^{m_0 \times m_0}: F \text{ is diagonal}, F^2 \le \gamma^{-2} I_{m_0}\} \tag{6}$$

If we additionally define

$$\mathcal{F}_M^- \triangleq \{F \in \mathcal{R}^{m_0 \times m_0}: F \text{ is diagonal}, -M \le F \le 0\} \tag{7}$$

then $F \in \mathcal{F}_M^+$ if and only if $-F \in \mathcal{F}_M^-$, and if $\gamma^{-1} = \sigma_{\max}(M)$, $F \in \mathcal{F}_\gamma$ implies $F \in \mathcal{F}_M^+ \cup \mathcal{F}_M^-$.

Now, denote $\tilde{G}(s)$ by

$$\tilde{G}(s) \sim \left[\begin{array}{c|c} \tilde{A} & \tilde{B}_0 \\ \hline \tilde{C}_0 & 0 \end{array}\right] \tag{8}$$

Then evaluation of the robust stability of Eq. (3) is equivalent to evaluation of the robust stability of the feedback system shown in Fig. 1.

It now follows that for asymptotically stable $\tilde{A} - \tilde{B}_0F\tilde{C}_0$ the $H_2$ norm for Eqs. (3) and (4) is given by

$$J(F) = \text{tr } \tilde{Q}\tilde{R} = \text{tr } \tilde{P}\tilde{V} \tag{9}$$

where

$$\tilde{R} = \tilde{E}^T\tilde{E} \tag{10}$$

$$\tilde{V} = \tilde{D}\tilde{D}^T \tag{11}$$

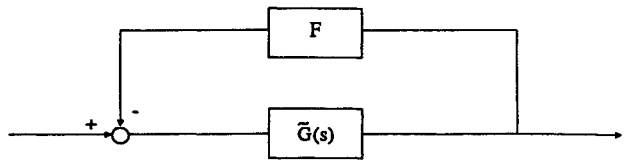


**Fig. 1 Feedback system to be analyzed for robust stability.**

$$0 = (\tilde{A} - \tilde{B}_0F\tilde{C}_0)^T\tilde{P} + \tilde{P}(\tilde{A} - \tilde{B}_0F\tilde{C}_0) + \tilde{R} \tag{12}$$

$$0 = (\tilde{A} - \tilde{B}_0F\tilde{C}_0)\tilde{Q} + \tilde{Q}(\tilde{A} - \tilde{B}_0F\tilde{C}_0)^T + \tilde{V} \tag{13}$$

If $w(t)$ is a standard white noise process with identity intensity, then $J(F) = \lim_{t\to\infty} \mathcal{E}[\tilde{x}^T(t)\tilde{R}\tilde{x}(t)]$. Later we will present robust performance bounds $\bar{J}$ such that $J(F) \le \bar{J}$ for each $F$ in the uncertainty set.

Next, we state the versions of the small gain, positivity, and Popov theorems that give sufficient conditions for the stability of the uncertain system (3) or, equivalently, the negative feedback interconnection of Fig. 1. Each of the theorems includes both a frequency domain test and an equivalent state-space test. In addition, robust $H_2$ performance bounds corresponding to the state-space tests are presented.

*Theorem 1 (Small Gain Theorem[7]).* If $(1/\gamma)\tilde{G}(s)$ is strictly bounded real, then the negative feedback interconnection of $\tilde{G}(s)$ and $F$ is asymptotically stable for all $F \in \mathcal{F}_\gamma$. Equivalently, if for any symmetric, positive definite $\tilde{R}$ there exists a positive scalar $\alpha$ and nonnegative definite $P$ satisfying

$$0 = \tilde{A}^TP + P\tilde{A} + \gamma^{-2}P\tilde{B}_0\tilde{B}_0^TP + \tilde{C}_0^T\tilde{C}_0 + \alpha\tilde{R} \tag{14}$$

then the uncertain system (3) is asymptotically stable for all $F \in \mathcal{F}_\gamma$. In this case, for all $F \in \mathcal{F}_\gamma$,

$$J(F) \le \bar{J}(\alpha) = (1/\alpha)\text{tr}(P\tilde{V}) \tag{15}$$

*Theorem 2 (Positivity Theorem[7]).* If $M^{-1} + \tilde{G}(s)$ is strongly positive real, then the negative feedback interconnection of $\tilde{G}(s)$ and $F$ is asymptotically stable for all $F \in \mathcal{F}_M^+$. Equivalently, if for any symmetric, positive definite $\tilde{R}$ there exists a positive scalar $\alpha$ and nonnegative definite $P$ satisfying

$$0 = \tilde{A}^TP + P\tilde{A} + \tfrac{1}{2}(\tilde{C}_0 - \tilde{B}_0^TP)^TM^{-1}(\tilde{C}_0 - \tilde{B}_0^TP) + \alpha\tilde{R} \tag{16}$$

then the uncertain system (3) is asymptotically stable for all $F \in \mathcal{F}_M^+$. In this case, for all $F \in \mathcal{F}_M^+$,

$$J(F) \le \bar{J}(\alpha) = (1/\alpha)\text{tr}(\tilde{P}\tilde{V}) \tag{17}$$

*Theorem 3 (Popov Theorem[6,7]).* If there exists a non-negative-definite diagonal matrix $N$ such that $M^{-1} + (I + N\tilde{s})\tilde{G}(s)$ is strongly positive real, then the negative feedback interconnection of $\tilde{G}(s)$ and $F$ is asymptotically stable for all $F \in \mathcal{F}_M^+$. Equivalently, if for any symmetric, positive definite $\tilde{R}$ there exists a nonnegative-definite diagonal matrix $N$, a positive scalar $\alpha$ and nonnegative-definite $P$ satisfying

$$0 = \tilde{A}^TP + P\tilde{A} + (\tilde{C}_0 + N\tilde{C}_0\tilde{A} - \tilde{B}_0^TP)^T[(M^{-1} + N\tilde{C}_0\tilde{B}_0)$$

$$+ (M^{-1} + N\tilde{C}_0\tilde{B}_0)^T]^{-1}(\tilde{C}_0 + N\tilde{C}_0\tilde{A} - \tilde{B}_0^TP) + \alpha\tilde{R} \tag{18}$$

then the uncertain system (3) is asymptotically stable for all $F \in \mathcal{F}_M^+$. In this case, for all $F \in \mathcal{F}_M^+$,

$$J(F) \le \bar{J}(\alpha, N) = (1/\alpha)\text{tr}((P + \tilde{C}_0^TMN\tilde{C}_0)\tilde{V}) \tag{19}$$

*Remark 1.* Theorem 2 may be considered a special case of Theorem 3 with $N = 0$.

*Remark 2.* In each of the three theorems the requirement that $\tilde{R}$ be positive definite can be relaxed. In particular, $\tilde{R}$ is

allowed to be nonnegative definite as long as the pair $(\tilde{A}, \tilde{E})$ is detectable where $\tilde{E}$ satisfies $\tilde{E}^T\tilde{E} = \tilde{R}$.

*Remark 3.* For the case of scalar uncertainty $F$ (i.e., $m_0 = 1$), the frequency domain tests given in the three theorems have easy-to-implement graphical frequency domain interpretations.[2]

*Remark 4.* As shown in Ref. 7, the Lyapunov function that establishes robust stability of the negative feedback interconnection of $\tilde{G}(s)$ and $F$ in Theorems 1 and 2 is a fixed Lyapunov function of the form $V(\tilde{x}) = \tilde{x}^TP\tilde{x}$ where $P$ satisfies Eqs. (14) and (16), respectively. On the other hand, the Lyapunov function that establishes robust stability of the negative feedback interconnection of $\tilde{G}(s)$ and $F$ in Theorem 3 is a parameter-dependent Lyapunov function; that is, it is a function of the uncertain parameters and has the form $V(\tilde{x}) = \tilde{x}^TP\tilde{x} + \tilde{x}^T\tilde{C}_0^TFN\tilde{C}_0\tilde{x}$ where $P$ satisfies Eq. (18).

*Remark 5.* Note that the Popov multiplier $N$ can be a negative-definite diagonal matrix that in the single-input/single-output (SISO) case simply corresponds to a Popov line in the Popov plane with a negative slope.[2] In this case, we note that the candidate Lyapunov function has the form $V(\tilde{x}) = \tilde{x}^TP\tilde{x} - \tilde{x}^T\tilde{C}_0^TF\hat{N}\tilde{C}_0\tilde{x}$, where $\hat{N} > 0$. Hence, it is necessary to check a posteriori the positive definiteness of $V(\tilde{x})$ for all $F \in F_M^+$ to insure that $V(\tilde{x})$ is a Lyapunov function.

*Remark 6.* An alternative statement of Theorem 3 that directly captures uncertainty $F \in F_M^+ \cup F_M^-$ can be obtained by considering the multivariable shifted Popov theorem.[9] Specifically, this case corresponds to replacing $M$ with $2M$ and $\tilde{A}$ with $\tilde{A} - \tilde{B}_0M\tilde{C}_0$ in Theorem 3. In this case the frequency domain interpretation for the case of scalar uncertainty involves a family of frequency-dependent off-axis circles in the Nyquist plane. The circle centers vary as a function of the phase of the Popov multiplier, but each has the same real axis intercepts at $\pm M^{-1}$. For further details see Refs. 9–11.

## III. Benchmark Two-Mass/Spring Example

Consider the two-mass/spring system shown in Fig. 2 with uncertain stiffness $k$. A control force acts on body 1, and the position of body 2 is measured, resulting in a noncollocated control problem. Here, we consider controller 1 of Ref. 8, which was designed for problem 1 of a benchmark problem[12] using the maximum entropy robust control design technique. The controller transfer function given by

$$G_c(s) = \frac{194390(s + 0.33679)[(s - 0.11735)^2 + 0.90996^2]}{(s + 81.438)(s + 131.04)[(s + 2.9049)^2 + 1.8615^2]} \quad (20)$$

was designed so that the closed-loop system is robust with respect to perturbations in the nominal value of the stiffness $k$ (i.e., $k = k_{\text{nom}}$). The exact stiffness stability region over which the system will remain stable was computed by a simple search and is given by

$$0.4458 < k < 2.0661 \quad (21)$$

Next, using a graphical approach and the state-space Riccati equation approach, we apply small gain analysis, positivity analysis, and Popov analysis to determine the stiffness stability regions predicted by each of these tests. Each of these tests is related to the previous test and is guaranteed to be less conservative.

We begin by constructing the uncertainty feedback system that will be used in each of the tests. The open-loop plant (for $m_1 = m_2 = 1$) is given by

$$\dot{x}(t) = A(k)x(t) + Bu(t) + D_1w(t) \quad (22a)$$

$$y(t) = Cx(t) + D_2w(t) \quad (22b)$$

$$z(t) = E_1x(t) \quad (22c)$$

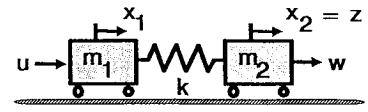


**Fig. 2 Benchmark two-mass/spring system for robust control design and analysis.**

where

$$A(k) = \begin{bmatrix} 0 & 0 & 1 & 0 \\ 0 & 0 & 0 & 1 \\ -k & k & 0 & 0 \\ k & -k & 0 & 0 \end{bmatrix}, \quad B = \begin{bmatrix} 0 \\ 0 \\ 1 \\ 0 \end{bmatrix}$$

$$D_1 = \begin{bmatrix} 0 & 0 \\ 0 & 0 \\ 0 & 0 \\ 1 & 0 \end{bmatrix}, \quad C = E_1 = [0\ 1\ 0\ 0], \quad D_2 = [0\ 1] \quad (23)$$

The $H_2$ cost functional under consideration is defined with respect to the transfer function between the disturbance $w(t)$ and the performance vector $z(t) + E_2u(t)$, where $E_2 = \sqrt{10^{-5}}$. The perturbation in $A(k)$ due to a change in the stiffness element $k$ from the nominal value $k_{\text{nom}}$ is given by

$$A(k) - A(k_{\text{nom}}) \triangleq \Delta A = -B_0\Delta kC_0 \quad (24)$$

where

$$B_0 = \begin{bmatrix} 0 \\ 0 \\ 1 \\ -1 \end{bmatrix}, \quad C_0 = [1\ -1\ 0\ 0] \quad (25)$$

In the subsequent analysis we will choose $k_{\text{nom}} = 0.6$ since the controller (20) was developed under this assumption.

Let the triple $(A_c, B_c, C_c)$ denote the state-space representation of the controller (20). Then, assuming negative feedback, the closed-loop state matrix is given by

$$\tilde{A}(k) = \begin{bmatrix} A(k) & -BC_c \\ B_cC & A_c \end{bmatrix} \quad (26)$$

In addition, $\tilde{R}$ and $\tilde{V}$ are given by Eqs. (10) and (11) where

$$\tilde{E} = [E_1\ -E_2C_c], \quad \tilde{D} = \begin{bmatrix} D_1 \\ B_cD_2 \end{bmatrix} \quad (27)$$

Next, define

$$\tilde{B}_0 = \begin{bmatrix} B_0 \\ 0_{4\times 1} \end{bmatrix}, \quad \tilde{C}_0 = [C_0\ \ 0_{1\times 4}] \quad (28)$$

and recall

$$\tilde{G}(s) \sim \left[\begin{array}{c|c} \tilde{A} & \tilde{B}_0 \\ \hline \tilde{C}_0 & 0 \end{array}\right] \quad (29)$$

Then, the plant uncertainty $\Delta k$ can be represented by the fictitious feedback loop shown in Fig. 1 with $F = \Delta k$. Notice that with this stiffness uncertainty $\tilde{C}_0\tilde{B}_0 = 0$, which holds for any state-space realization of the system.

## IV. Frequency Domain Graphical Analysis of the Benchmark System

In this section we apply the frequency domain tests described in the three theorems of Sec. II to determine $\overline{\Delta k}$ (positive) and $\underline{\Delta k}$ (negative) such that stability is guaranteed for

$$k_{\text{nom}} + \underline{\Delta k} < k < k_{\text{nom}} + \overline{\Delta k} \quad (30)$$

Since the uncertainty is scalar, we will first use the graphical techniques derived from the frequency domain tests. These graphical tests originally appeared in Refs. 13 and 14 and are included here for comparison with the results based on the state-space formulations.

**Small Gain Analysis**

Small gain analysis requires considering the Nyquist diagram of $\tilde{G}(s)$. The smallest circle centered at the origin that completely encompasses the Nyquist diagram, $\mathrm{Im}[\tilde{G}(j\omega)]$ vs $\mathrm{Re}[\tilde{G}(j\omega)]$ for all $\omega$, (without touching it) is then drawn. The intersection of this circle with the negative real axis is given by $-1/\Delta k$, and the intersection with the positive real axis is given by $-1/\underline{\Delta k}$. This analysis is shown in Fig. 3. It follows that $\Delta k = 0.1497$ and $\underline{\Delta k} = -0.1497$. Hence, using small gain analysis, stability is guaranteed for

$$0.4503 < k < 0.7497 \tag{31}$$

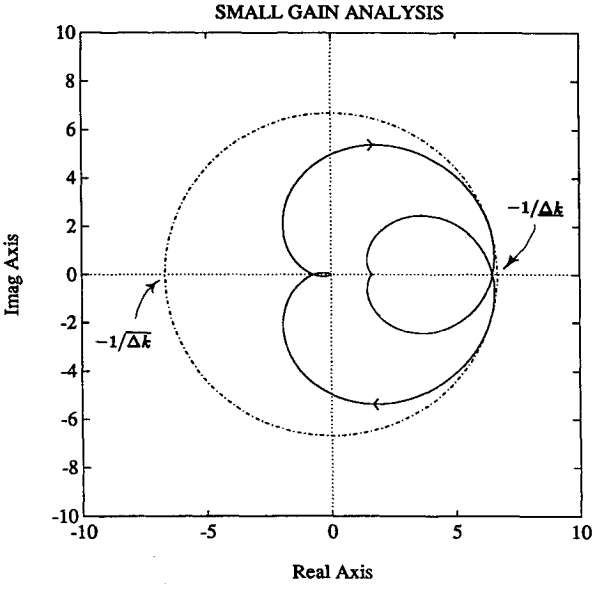


**Fig. 3 Frequency domain small gain analysis.**

Note that since the $\Delta k$ uncertainty block is composed of a single scalar, this result is equivalent to the complex structured singular value test.[15]

**Positivity Analysis**

Positivity analysis determines stability bounds by drawing straight-lines that lie to the left or right of the Nyquist diagram (without touching it). For the Nyquist diagram of $\tilde{G}(s)$, the intersection of the line to the left of the Nyquist plot with the negative real axis equals $-1/\Delta k$. The intersection of the line to the right of the Nyquist plot with the positive real axis equals $-1/\underline{\Delta k}$. This analysis is shown in Fig. 4. It follows that $\Delta k = 0.5278$ and $\underline{\Delta k} = -0.1523$. Hence, using positivity analysis, stability is guaranteed for

$$0.4477 < k < 1.1278 \tag{32}$$

**Popov Analysis**

Popov analysis is a test that determines a stability bound from a modified Nyquist diagram, namely, the Popov plot, $\omega\ \mathrm{Im}[\tilde{G}(j\omega)]$ vs $\mathrm{Re}[\tilde{G}(j\omega)]$ for $\omega \geq 0$. This analysis requires finding lines (Popov lines) that intersect the negative or positive real axis at a point that is to the left of the Popov plot but as close to the origin as possible. The slopes of these lines are $-1/\overline{N}$ and $-1/\underline{N}$ where $\overline{N}$ and $\underline{N}$ are the Popov multipliers. The Popov test is equivalent to the positive real test if the lines are chosen to be vertical. For the Popov diagram of $\tilde{G}(s)$, the intersection of the line to the left of the Popov plot with the negative real axis equals $-1/\Delta k$. The intersection of the line to the right of the Popov plot with the positive real axis equals $-1/\underline{\Delta k}$. This analysis is shown in Fig. 5. It follows that $\Delta k = 1.4661$ and $\underline{\Delta k} = 0.1542$, and the corresponding Popov multipliers are, respectively, $\overline{N}^* = 0.7999$ and $\underline{N}^* = -0.2755$. Hence, using Popov analysis, one guarantees stability for

$$0.4458 < k < 2.0661 \tag{33}$$

Note that these bounds are identical to the exact bounds of Eq. (21). Hence, for this example, Popov analysis yields totally nonconservative robust stability results. This is not surprising since, as mentioned in the Introduction, the Popov result is based on a parameter-dependent Lyapunov function that severely restricts the allowable time variation of the uncertain parameters and hence closely approximates real parameter uncertainty within robustness analysis.

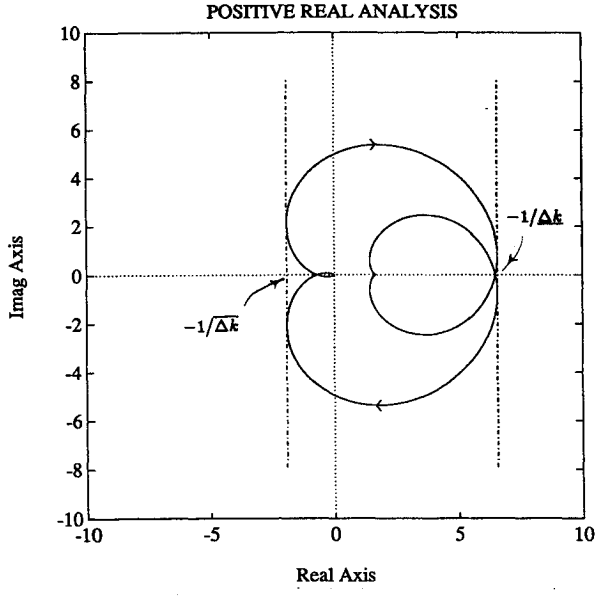


**Fig. 4 Frequency domain positivity analysis.**

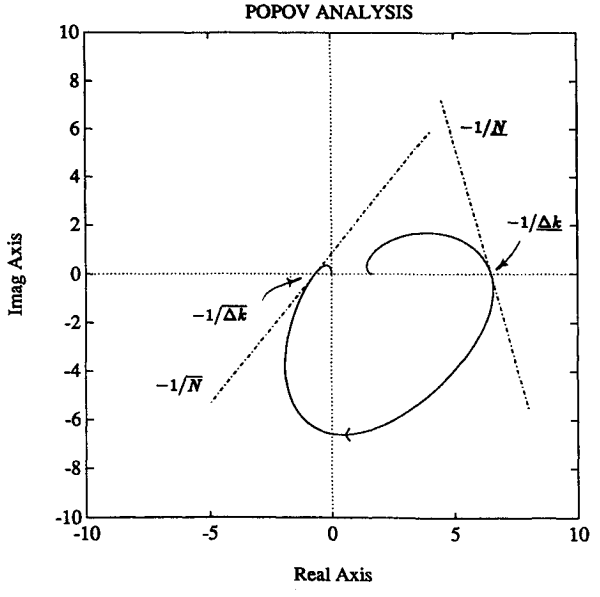


**Fig. 5 Frequency domain Popov analysis.**

## V. State-Space Analysis of the Benchmark System

Continuation (or homotopy) algorithms[16,17] are effective techniques for solving systems of nonlinear algebraic equations and have found increasing engineering applications (see, for example, Refs. 17-19). In this section, we develop continuation algorithms that implement the state-space analysis results described in the three theorems of Sec. II. We restrict ourselves to the case of scalar uncertainty (i.e., $F$ is a scalar) with $\tilde{C}_0\tilde{B}_0 = 0$ (which applies to the benchmark system). In addition, the exposition is focused on implementing state-space Popov analysis since this case is the most complex. The algorithms for small gain and positivity analyses are very similar and hence are only briefly discussed. The results of applying these algorithms to the benchmark problem are subsequently presented.

Each of the algorithms is based on optimizing the cost upper bounds $\bar{J}$ of Eqs. (15), (17), and (19). At this point we focus attention on the upper bound, Eq. (19), of the Popov theorem, rewritten here for all $F \in \boldsymbol{F}_M^+$ as

$$\bar{J}(\alpha, N) \triangleq (1/\alpha)\mathrm{tr}((P + \tilde{C}_0^T M N \tilde{C}_0)\tilde{V}) \tag{34}$$

where, for $\tilde{C}_0\tilde{B}_0 = 0$, $P$ is given by

$$0 = \tilde{A}^T P + P\tilde{A} + (\tfrac{1}{2})(\tilde{C}_0 + N\tilde{C}_0\tilde{A} - \tilde{B}_0^T P)^T M(\tilde{C}_0 + N\tilde{C}_0\tilde{A} - \tilde{B}_0^T P) + \alpha\tilde{R} \tag{35}$$

The algorithm under consideration will be based on finding scalars $\alpha$ and $N$ that satisfy

$$0 = \frac{\partial \bar{J}}{\partial \alpha} = \mathrm{tr}(Q\tilde{R} - \frac{1}{\alpha^2}(P\tilde{V} + \tilde{C}_0^T M N \tilde{C}_0 \tilde{V})) \tag{36}$$

$$0 = \frac{\partial \bar{J}}{\partial N} = \frac{1}{\alpha} M\tilde{C}_0\tilde{V}\tilde{C}_0^T + M(\tilde{C}_0 + N\tilde{C}_0\tilde{A} - \tilde{B}_0^T P)Q\tilde{A}^T\tilde{C}_0^T \tag{37}$$

where $Q$ satisfies

$$0 = (A - \tfrac{1}{2}\tilde{B}_0 M(\tilde{C}_0 + N\tilde{C}_0\tilde{A} - \tilde{B}_0^T P))Q + Q(A - \tfrac{1}{2}\tilde{B}_0 M(\tilde{C}_0 + N\tilde{C}_0\tilde{A} - \tilde{B}_0^T P))^T + (1/\alpha)\tilde{V} \tag{38}$$

### Continuation Map for Popov Analysis

To define the continuation map we assume that the uncertainty parameter $M$ is a function of the continuation parameter $\lambda \in [0, 1]$. In particular, it is assumed that

$$M(\lambda) = M_0 + \lambda(M_f - M_0) \tag{39}$$

Note that, at $\lambda = 0$, $M(\lambda) = M_0$, whereas at $\lambda = 1$, $M(\lambda) = M_f$. The continuation map is defined as the gradient of the upper bound on the cost for the uncertainty parameter $M(\lambda)$. In particular,

$$H(\theta, \lambda) \triangleq \begin{bmatrix} H_1(\theta, \lambda) \\ H_2(\theta, \lambda) \end{bmatrix} \tag{40}$$

where

$$\theta \triangleq \begin{bmatrix} \alpha \\ N \end{bmatrix} \tag{41}$$

$$H_1(\theta, \lambda) \triangleq \mathrm{tr}(Q(\theta, \lambda)\tilde{R} - \frac{1}{\alpha(\lambda)^2}(P(\theta, \lambda)\tilde{V} + \tilde{C}_0^T M(\lambda) N(\lambda)\tilde{C}_0\tilde{V})) \tag{42}$$

$$H_2(\theta, \lambda) \triangleq \frac{1}{\alpha(\lambda)} M(\lambda)\tilde{C}_0\tilde{V}\tilde{C}_0^T + M(\lambda)(\tilde{C}_0 + N(\lambda)\tilde{C}_0\tilde{A} - \tilde{B}_0^T P(\theta, \lambda))Q(\theta, \lambda)\tilde{A}^T\tilde{C}_0^T \tag{43}$$

and

$$0 = \tilde{A}^T P(\theta, \lambda) + P(\theta, \lambda)\tilde{A} + \tfrac{1}{2}(\tilde{C}_0 + N(\lambda)\tilde{C}_0\tilde{A} - \tilde{B}_0^T P(\theta, \lambda))^T M(\lambda) \cdot (\tilde{C}_0 + N(\lambda)\tilde{C}_0\tilde{A} - \tilde{B}_0^T P(\theta, \lambda)) + \alpha(\lambda)\tilde{R} \tag{44}$$

$$0 = [\tilde{A} - \tfrac{1}{2}\tilde{B}_0 M(\lambda)(\tilde{C}_0 + N(\lambda)\tilde{C}_0\tilde{A} - \tilde{B}_0^T P(\theta, \lambda))]Q(\theta, \lambda) + Q(\theta, \lambda)[\tilde{A} - \tfrac{1}{2}\tilde{B}_0 M(\lambda)(\tilde{C}_0 + N(\lambda)\tilde{C}_0\tilde{A} - \tilde{B}_0^T P(\theta, \lambda))]^T + \frac{1}{\alpha(\lambda)}\tilde{V} \tag{45}$$

The continuation curve is defined by

$$0 = H(\theta, \lambda), \qquad \lambda \in [0, 1] \tag{46}$$

### Jacobian of the Continuation Map for Popov Analysis

The algorithm requires computation of $\nabla H(\theta, \lambda)^T$, the Jacobian of $H(\theta, \lambda)$. Note that

$$\nabla H(\theta, \lambda)^T = [H_\theta \; H_\lambda] \tag{47}$$

where

$$H_\theta \triangleq \frac{\partial H}{\partial \theta} \tag{48a}$$

$$H_\lambda \triangleq \frac{\partial H}{\partial \lambda} \tag{48b}$$

Expressions for $H_\theta$ and $H_\lambda$ are given in the Appendix.

### Outline of the Continuation Algorithm for Popov Analysis

Step 1. Initialize $loop = 0$, $\lambda = 0$, $\Delta\lambda \in [0, 1]$, $\theta^T = [1\ 0]$ (i.e., $\alpha = 1$, $N = 0$).

Step 2. Let $loop = loop + 1$. If $loop = 1$, then go to step 4. Otherwise, continue.

Step 3. Advance the homotopy parameter and predict the corresponding parameter vector $\theta$ as follows.

3a. Let $\lambda_0 = \lambda$.

3b. Let $\lambda = \lambda_0 + \Delta\lambda$.

3c. Compute $H_\theta(\theta, \lambda)$ and $H_\lambda(\theta, \lambda)$. Then compute $\theta_p'(\lambda_0)$ using

$$\theta_p'(\lambda_0) = -[H_\theta(\theta, \lambda)]^{-1}H_\lambda(\theta, \lambda_0) \tag{49}$$

3d. Predict $\theta(\lambda)$ using $\theta(\lambda) = \theta(\lambda_0) + \Delta\lambda\theta_p'(\lambda_0)$.

3e. If $\|H(\theta, \lambda)\|$ satisfies some preassigned prediction tolerance, then continue. Otherwise, reduce $\Delta\lambda$ and go to step 3b.

Step 4. Correct the current approximation $\theta(\lambda)$ as follows.

4a. Compute $H(\theta, \lambda)$ and $H_\theta(\lambda)$.

4b. Correct $\theta(\lambda)$ using $\theta(\lambda) \leftarrow \theta(\lambda) - [H_\theta(\theta, \lambda)]^{-1}H(\theta, \lambda)$.

4c. If $\|H(\theta, \lambda)\|$ satisfies some preassigned tolerance, then continue. Otherwise, go to step 4a.

4d. If $P(\lambda)$ is not nonnegative definite, then go to step 5, since stability is only guaranteed for $M = M(\lambda_0)$. Otherwise, continue.

4e. Compute the upper bound $\bar{J}(\theta)$.

4f. If $\lambda = 1$, then continue. Otherwise, go to step 2.

Step 5. Stop.

### Continuation Algorithm for Positivity Analysis

Recall that positivity analysis is a special case of Popov analysis (with $N \triangleq 0$). Hence, positivity analysis is implemented using the algorithm for Popov analysis with $N$ constrained to zero.

**Continuation Algorithm for Small Gain Analysis**

For small gain analysis we consider the upper bound $\bar{J}(\alpha)$ of Eq. (15), rewritten here as

$$\bar{J}(\alpha) \triangleq (1/\alpha)\mathrm{tr}(P\tilde{V}) \tag{50}$$

where

$$0 = \tilde{A}^T P + P\tilde{A} + M^{-2}P\tilde{B}_0\tilde{B}_0^T P + \tilde{C}_0^T\tilde{C}_0 + \alpha\tilde{R} \tag{51}$$

The algorithm is based on finding a scalar $\alpha$ such that

$$0 = \frac{\partial \bar{J}}{\partial \alpha} = \mathrm{tr}\left(Q\tilde{R} - \frac{1}{\alpha^2}P\tilde{V}\right) \tag{52}$$

where $Q$ satisfies

$$0 = (\tilde{A} + M^{-2}\tilde{B}_0\tilde{B}_0^T P)Q + Q(\tilde{A} + M^{-2}\tilde{B}_0\tilde{B}_0^T P)^T + (1/\alpha)\tilde{V} \tag{53}$$

It is assumed that $M(\lambda)$ is as given by Eq. (39) and the continuation map is defined as

$$H(\theta, \lambda) = \mathrm{tr}\left(Q(\theta, \lambda)\tilde{R} - \frac{1}{\alpha^2}P(\theta, \lambda)\tilde{V}\right) \tag{54}$$

where

$$\theta \triangleq \alpha \tag{55}$$

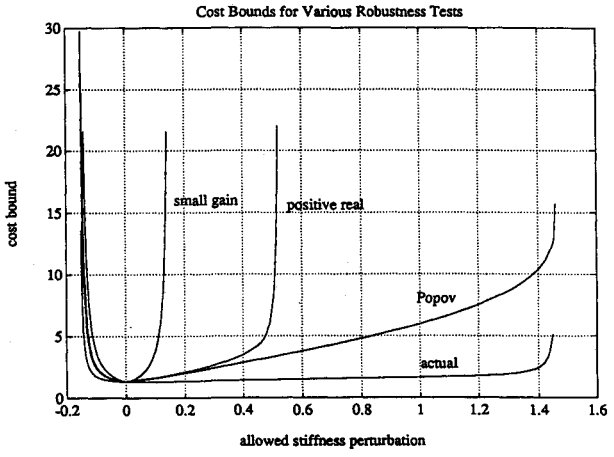


**Fig. 6 Performance bounds for the small gain, positivity, and Popov tests.**

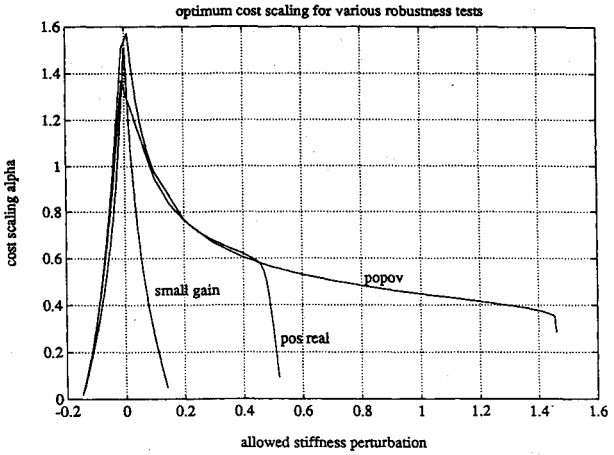


**Fig. 7 Optimal $\alpha$ for the small gain, positivity, and Popov tests.**

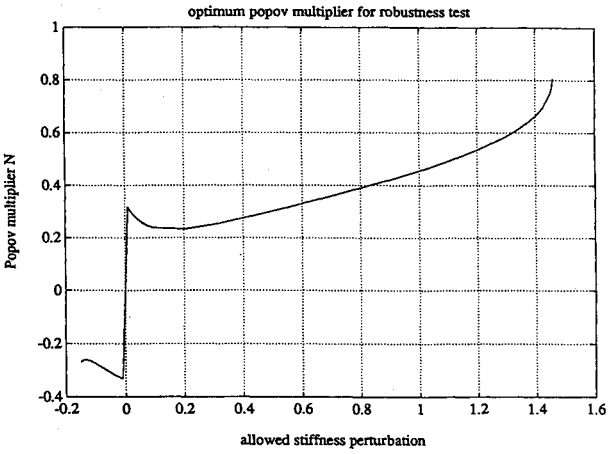


**Fig. 8 Optimal $N$ for the Popov test.**

$$0 = \tilde{A}^T P(\theta, \lambda) + P(\theta, \lambda)\tilde{A} + M(\lambda)^{-2}P(\theta, \lambda)\tilde{B}_0\tilde{B}_0^T P(\theta, \lambda) + \tilde{C}_0^T\tilde{C}_0 + \alpha\tilde{R} \tag{56}$$

$$0 = (\tilde{A} + M(\lambda)^{-2}\tilde{B}_0\tilde{B}_0^T P(\theta, \lambda))Q(\theta, \lambda) + Q(\theta, \lambda)(\tilde{A} + M(\lambda)^{-2}\tilde{B}_0\tilde{B}_0^R P(\theta, \lambda))^T + (1/\alpha)\tilde{V} \tag{57}$$

The continuation curve is defined by

$$0 = H(\theta, \lambda), \qquad \lambda \in [0, 1] \tag{58}$$

Expressions for the Hessian $H_\theta$ and $H_\lambda$ are given in the Appendix.

The outline of the continuation algorithm for small gain analysis is identical to that given for Popov analysis. Because of this, no further discussion is needed.

**Analysis of the Benchmark Problem**

When the continuation algorithms for small gain, positivity, and Popov analysis are applied to the benchmark problem, the performance curves shown in Fig. 6 result. As expected, Popov analysis yields less conservative results than the positivity and small gain tests. The robust stability bounds $\overline{\Delta k}$ (positive) and $\underline{\Delta k}$ (negative) obtained from the state-space tests are identical to those obtained from the frequency domain tests of Sec. IV. The optimal $\alpha$ for each test is shown in Fig. 7 as a function of $M$. The optimal $N$ for the Popov test is shown in Fig. 8. Note that as $M$ approaches its supremum and infimum, $N$ converges, respectively, to $\overline{N}^*$ and $\underline{N}^*$ obtained from the graphical test.

## VI. Conclusions

This paper has discussed the small gain, positivity, and Popov tests and applied both the (graphical) frequency domain version of each test and the corresponding state-space test to a benchmark problem. The frequency domain tests and the state-space tests were seen to give identical results for robust stability, and the Popov test was completely nonconservative in its robustness predictions. The state-space tests also yielded robust $H_2$ performance bounds and were implemented using continuation algorithms. The algorithms developed here only apply to the special case of scalar uncertainty and the algorithm for the Popov test further requires that a certain product (related to the uncertainty pattern) is zero. Future work will involve the development of more general numerical algorithms.

## Appendix: Jacobian Expressions for the Popov and Small Gain Tests

In this Appendix we show how to compute the Jacobian of the homotopy map $H(\theta, \lambda)$ for both the Popov and small gain

tests. We first recall that the Jacobian $\nabla H(\theta, \lambda)$ is defined by

$$\nabla H(\theta, \lambda)^T \triangleq [H_\theta, H_\lambda] \tag{A1}$$

where

$$H_\theta \triangleq \frac{\partial H}{\partial \theta}, \qquad H_\lambda \triangleq \frac{\partial H}{\partial \lambda} \tag{A2}$$

Since $H(\theta, \lambda)$ corresponds to the upper bounds of the cost corresponding to $M(\lambda)$, $H_\theta$ is the corresponding Hessian.

**Jacobian Expressions for Popov Analysis**

$$H_\theta = \begin{bmatrix} \frac{\partial}{\partial \alpha} H_1(\theta, \lambda) & \frac{\partial}{\partial N} H_1(\theta, \lambda) \\ \text{SYM} & \frac{\partial}{\partial N} H_2(\theta, \lambda) \end{bmatrix} \tag{A3}$$

where

$$\frac{\partial}{\partial \alpha} H_1 = \operatorname{tr}\left( \frac{\partial Q}{\partial \alpha} \tilde{R} - \frac{1}{\alpha^2} \frac{\partial P}{\partial \alpha} \tilde{V} + \frac{2}{\alpha^3} (P \tilde{V} + \tilde{C}_0^T M N \tilde{C}_0 \tilde{V}) \right) \tag{A4}$$

$$\frac{\partial}{\partial N} H_2 = \left( -M \tilde{B}_0^T \frac{\partial P}{\partial N} Q + M(\tilde{C}_0 + N \tilde{C}_0 \tilde{A} - \tilde{B}_0^T P) \frac{\partial Q}{\partial N} + M \tilde{C}_0 \tilde{A} Q) \tilde{A}^T \tilde{C}_0^T \right) \tag{A5}$$

$$\frac{\partial}{\partial N} H_1 = \operatorname{tr}\left( \frac{\partial Q}{\partial N} \tilde{R} - \frac{1}{\alpha^2} \frac{\partial P}{\partial N} \tilde{V} - \frac{1}{\alpha^2} \tilde{C}_0^T M \tilde{C}_0 \tilde{V} \right) \tag{A6}$$

and $\partial P/\partial \alpha$, $\partial P/\partial N$, $\partial Q/\partial \alpha$, and $\partial Q/\partial N$ satisfy

$$0 = \tilde{A}_a^T \frac{\partial P}{\partial \alpha} + \frac{\partial P}{\partial \alpha} \tilde{A}_a + \tilde{R} \tag{A7}$$

$$0 = \tilde{A}_a^T \frac{\partial P}{\partial N} + \frac{\partial P}{\partial N} \tilde{A}_a + \tfrac{1}{2}[(\tilde{C}_0 + N \tilde{C}_0 \tilde{A} - \tilde{B}_0^T P)^T M \tilde{C}_0 \tilde{A} + \tilde{A}^T \tilde{C}_0^T M (\tilde{C}_0 + N \tilde{C}_0 \tilde{A} - B_0^T P)] \tag{A8}$$

$$0 = \tilde{A}_a \frac{\partial Q}{\partial \alpha} + \frac{\partial Q}{\partial \alpha} \tilde{A}_a^T + \left( \frac{1}{2} \tilde{B}_0 M \tilde{B}_0^T \frac{\partial P}{\partial \alpha} \right) Q + Q \left( \frac{1}{2} \tilde{B}_0 M \tilde{B}_0^T \frac{\partial P}{\partial \alpha} \right)^T - \frac{1}{\alpha^2} \tilde{V} \tag{A9}$$

$$0 = \tilde{A}_a \frac{\partial Q}{\partial N} + \frac{\partial Q}{\partial N} \tilde{A}_a^T + \left( \frac{1}{2} \tilde{B}_0 M \tilde{B}_0^T \frac{\partial P}{\partial N} \right) Q + Q \left( \frac{1}{2} \tilde{B}_0 M \tilde{B}_0^T \frac{\partial P}{\partial N} \right)^T - \left( \frac{1}{2} \tilde{B}_0 M \tilde{C}_0 \tilde{A} \right) Q - Q \left( \frac{1}{2} \tilde{B}_0 M \tilde{C}_0 \tilde{A} \right)^T \tag{A10}$$

where

$$\tilde{A}_a \triangleq \tilde{A} - \tfrac{1}{2} \tilde{B}_0 M (\tilde{C}_0 + N \tilde{C}_0 \tilde{A} - \tilde{B}_0^T P) \tag{A11}$$

Similarly, $H_\lambda$ is given by

$$H_\lambda = \begin{bmatrix} \frac{\partial}{\partial \lambda} H_1(\theta, \lambda) \\ \frac{\partial}{\partial \lambda} H_2(\theta, \lambda) \end{bmatrix} \tag{A12}$$

where

$$\frac{\partial}{\partial \lambda} H_1 = \operatorname{tr}\left( \frac{\partial Q}{\partial \lambda} \tilde{R} - \frac{1}{\alpha^2} \left( \frac{\partial P}{\partial \lambda} \tilde{V} + \tilde{C}_0^T (M_f - M_0) N \tilde{C}_0 \tilde{V} \right) \right) \tag{A13}$$

$$\frac{\partial}{\partial \lambda} H_2 = \frac{1}{\alpha} (M_f - M_0) \tilde{C}_0 \tilde{V} \tilde{C}_0^T + \left[ (M_f - M_0)(\tilde{C}_0 + N \tilde{C}_0 \tilde{A} - \tilde{B}_0^T P) Q - M \tilde{B}_0^T \frac{\partial P}{\partial \lambda} Q + M (\tilde{C}_0 + N \tilde{C}_0 \tilde{A} - \tilde{B}_0^T P) \frac{\partial Q}{\partial \lambda} \right] \tilde{A}^T \tilde{C}_0^T \tag{A14}$$

and $\partial P/\partial \lambda$ and $\partial Q/\partial \lambda$ satisfy

$$0 = \tilde{A}_a^T \frac{\partial P}{\partial \lambda} + \frac{\partial P}{\partial \lambda} \tilde{A}_a + \tfrac{1}{2} (\tilde{C}_0 + N \tilde{C}_0 \tilde{A} - \tilde{B}_0^T P)(M_f - M_0)(\tilde{C}_0 + N \tilde{C}_0 \tilde{A} - \tilde{B}_0^T P) \tag{A15}$$

$$0 = \tilde{A}_a \frac{\partial Q}{\partial \lambda} + \frac{\partial Q}{\partial \lambda} \tilde{A}_a^T + \left( \frac{1}{2} \tilde{B}_0 M \tilde{B}_0^T \frac{\partial P}{\partial \lambda} \right) Q + Q \left( \frac{1}{2} \tilde{B}_0 M \tilde{B}_0^T \frac{\partial P}{\partial \lambda} \right)^T - \left[ \frac{1}{2} \tilde{B}_0 (M_f - M_0)(\tilde{C}_0 + N \tilde{C}_0 \tilde{A} - \tilde{B}_0^T P) \right] Q - Q \left[ \frac{1}{2} \tilde{B}_0 (M_f - M_0)(\tilde{C}_0 + N \tilde{C}_0 \tilde{A} - \tilde{B}_0^T P) \right] \tag{A16}$$

**Jacobian Expressions for Small Gain Analysis**

The Hessian $H_\theta (\triangleq \partial H/\partial \theta)$ is given by

$$H_\theta = \operatorname{tr}\left( \frac{\partial Q}{\partial \alpha} \tilde{R} - \frac{1}{\alpha^2} \frac{\partial P}{\partial \alpha} \tilde{V} + \frac{2}{\alpha^3} P \tilde{V} \right) \tag{A17}$$

where $\partial P/\partial \alpha$ and $\partial Q/\partial \alpha$ satisfy

$$0 = \tilde{A}^T \frac{\partial P}{\partial \alpha} + \frac{\partial P}{\partial \alpha} \tilde{A} + \tilde{R} \tag{A18}$$

$$0 = (\tilde{A} + M^{-2} \tilde{B}_0 \tilde{B}_0^T P) \frac{\partial Q}{\partial \alpha} + \frac{\partial Q}{\partial \alpha} (\tilde{A} + M^{-2} \tilde{B}_0 \tilde{B}_0^T P)^T + M^{-2} \tilde{B}_0 \tilde{B}_0^T \frac{\partial P}{\partial \alpha} Q + \left( M^{-2} \tilde{B}_0 \tilde{B}_0^T \frac{\partial P}{\partial \alpha} Q \right)^T - \frac{1}{\alpha^2} \tilde{V} \tag{A19}$$

Similarly, $H_\lambda (\triangleq \partial H/\partial \lambda)$ is given by

$$H_\lambda = \operatorname{tr}\left( \frac{\partial Q}{\partial \lambda} \tilde{R} - \frac{1}{\alpha^2} \frac{\partial P}{\partial \lambda} \tilde{V} \right) \tag{A20}$$

where $\partial P/\partial \lambda$ and $\partial Q/\partial \lambda$ satisfy

$$0 = (\tilde{A} + M^{-2} \tilde{B}_0 \tilde{B}_0^T P)^T \frac{\partial P}{\partial \lambda} + \frac{\partial P}{\partial \lambda} (\tilde{A} + M^{-2} \tilde{B}_0 \tilde{B}_0^T P) - 2M^{-3} (M_f - M_0) P \tilde{B}_0 \tilde{B}_0^T P \tag{A21}$$

$$0 = (\tilde{A} + M^{-2} \tilde{B}_0 \tilde{B}_0^T P) \frac{\partial Q}{\partial \lambda} + \frac{\partial Q}{\partial \lambda} (\tilde{A} + M^{-2} \tilde{B}_0 \tilde{B}_0^T P)^T + M^{-2} \tilde{B}_0 \tilde{B}_0^T \frac{\partial P}{\partial \lambda} Q + \left( M^{-2} \tilde{B}_0 \tilde{B}_0^T \frac{\partial P}{\partial \lambda} Q \right)^T - 2M^{-3} (M_f - M_0)(\tilde{B}_0 \tilde{B}_0^T P Q + Q P \tilde{B}_0 \tilde{B}_0^T) \tag{A22}$$

## Acknowledgments

This research was supported in part by Sandia National Laboratories under Contract 54-7609, the Air Force Office of Scientific Research under Contract F49620-91-0019, the National Science Foundation under Grant ECS-91095588, and the Florida Space Grant Consortium under Grant NGT-40015.

## References

[1]Zames, G., "On the Input-Output Stability of Time-Varying Nonlinear Feedback Systems, Part I: Conditions Derived Using Concepts of Loop Gain, Conicity, and Positivity," *IEEE Transactions on Automatic Control*, Vol. AC-11, April 1966, pp. 228–238.

[2]Narendra, K. S., and Taylor, J. H., *Frequency Domain Criteria for Absolute Stability*, Academic Press, New York, 1973.

[3]Francis, B. A., and Doyle, J. C., "Linear Control Theory with an $H_\infty$ Optimality Criterion," *SIAM Journal of Control and Optimization*, Vol. 25, July 1987, pp. 815–844.

[4]Francis, B. A., *A Course in $H_\infty$ Control Theory*, Springer-Verlag, New York, 1987.

[5]Khargonekar, P. P., Petersen, I. R., and Zhou, K., "Robust Stabilization of Uncertain Linear Systems: Quadratic Stability and $H_\infty$ Theory," *IEEE Transactions on Automatic Control*, Vol. 35, March 1990, pp. 356–361.

[6]Haddad, W. M., and Bernstein, D. S., "Parameter-Dependent Lyapunov Functions, Constant Real Parameter Uncertainty, and the Popov Criterion in Robust Analysis and Synthesis: Part 1, Part 2," *Proceedings of the IEEE Conference on Decision and Control* (Brighton, England, UK), IEEE, Piscataway, NJ, 1991, pp. 2274–2279 and 2618–2623; also *IEEE Transactions on Automatic Control* (submitted for publication).

[7]Haddad, W. M., and Bernstein, D. S., "Explicit Construction of Quadratic Lyapunov Functions for the Small Gain, Positivity, Circle, and Popov Theorems and Their Application to Robust Stability, Part 1: Continuous-Time Theory, Part 2: Discrete-Time Theory," *International Journal on Robust and Nonlinear Control* (to be published).

[8]Collins, E. G., Jr., King, J. A., and Bernstein, D. S., "Application of Maximum Entropy/Optimal Projection Design Synthesis to a Benchmark Problem," *Journal of Guidance, Control, and Dynamics*, Vol. 15, No. 5, 1992, pp. 1094–1102.

[9]Haddad, W. M., and Bernstein, D. S., "The Multivariable Parabola Criterion for Robust Controller Synthesis: A Riccati Equation Approach," *Journal of Mathematical Systems, Estimation, and Control* (to be published).

[10]How, J. P., and Hall, S. R., "Connections Between the Popov Stability Criterion and Bounds for Real Parametric Uncertainty," *IEEE Transactions on Automatic Control* (submitted for publication).

[11]Haddad, W. M., How, J. P., Hall, S. R., and Bernstein, D. S., "Extensions of Mixed-$\mu$ Bounds to Monotonic and Odd Monotonic Nonlinearities Using Absolute Stability Theory," *International Journal of Control* (to be published).

[12]Wie, B., and Bernstein, D. S., "Benchmark Problems for Robust Control Design," *Journal of Guidance, Control, and Dynamics*, Vol. 25, No. 5, 1992, pp. 1057–1059.

[13]Collins, E. G., Jr., Haddad, W. M., and Bernstein, D. S., "Small Gain, Circle, Positivity, and Popov Analysis of a Maximum Entropy Controller for a Benchmark Problem," *Proceedings of the American Control Conference* (Chicago, IL), IEEE, Piscataway, NJ, 1991, pp. 2425–2426.

[14]Haddad, W. M., Collins, E. G., Jr., and Bernstein, D. S., "Robust Stability Analysis Using the Small Gain, Circle, Positivity, and Popov Theorems: A Comparative Study," *IEEE Transactions on Automatic Control Systems Technology*, Dec. 1993.

[15]Doyle, J. C., "Analysis of Feedback Systems with Structured Uncertainties," *IEE Proceedings, Part D*, Vol. 129, Nov. 1982, pp. 242–250.

[16]Watson, L. T., "Globally Convergent Homotopy Algorithms for Nonlinear Systems of Equations," *Nonlinear Dynamics*, Vol. 1, 1990, pp. 143–191.

[17]Richter, S. L., and DeCarlo, R. A., "Continuation Methods: Theory and Applications," *IEEE Transactions on Automatic Control*, Vol. CAS-30, No. 6, 1983, pp. 347–352.

[18]Lefebvre, S., Richter, S., and DeCarlo, R., "A Continuation Algorithm for Eigenvalue Assignment by Decentralized Constant-Output Feedback," *International Journal of Control*, Vol. 41, No. 5, 1985, pp. 1273–1292.

[19]Collins, E. G., Jr., Davis, L. D., and Richter, S., "A Homotopy Algorithm for Maximum Entropy Design," *Journal of Guidance, Control, and Dynamics* (to be published); also *Proceedings of the American Control Conference* (San Francisco, CA), IEEE, Piscataway, NJ, 1993, pp. 1010–1014.